Available in online @ www.iaraindia.com
SCIENCE EXPLORE-An International Journal on Science and Technology
Volume I, Issue 1
January – March 2026

SYNTHESIS AND CHARACTERIZATION OF Se-DOPED ZnO NANOCOMPOSITE MATERIAL AND ITS MULTI APPLICATIONS

J. SARAVANABAVA
PG & Research Department of Chemistry
Sri Vinayaga College of Arts and Science, Ulundurpet, Tamilnadu

R. GOPATHY
PG & Research Department of Chemistry
Arignar Anna Govt. Arts College, Cheyyar, Tiruvannamalai, Tamilnadu

JAYARAMAN KAMALAKKANNAN
PG and Research Department of Physics
Pachaiyappa's college , Chennai, Tamilnadu

ABSTRACT

An ZnO and Se- ZnO nanocomposite material was synthesized by a precipitation method. The obtained material was characterized by high resolution scanning electron microscopy (FE-SEM) with energy dispersive X-ray analysis (EDX), X-ray diffraction (XRD), photoluminescence spectroscopy (PL), UV visible diffuse reflectance spectroscopy (UV-Vis-DRS) analysis. The ZnO and Se- ZnO degradation of azo dye in Trypan Blue (TB) under solar irradiation for enhanced that of UV irradiation. ZnO and Se- ZnO is found to be reusable without appreciable loss of catalytic activity up to five runs its performance as an active photocatalyst very important industrial application material, The mechanism of the photocatalytic effect of the ZnO and Se - ZnO Al nanocomposite material has been discussed. The proposed use of ZnO and Se- ZnO in water purification technique is promising.

KEYWORDS*:* SEM, XRD,TEM Photocatalysis, reusable

INTRODUCTION

General Introduction Of Nanomaterial

Perspective Of Length nanomaterials been helped by the industrial ability and aims to manipulate nanomaterials whose dimensions are in nanometers. These have been labeled as new age nanomaterials. In order to understand the typical world of nanamaterials and nanotechnology, we require finding an idea of unit of measure drawn in. The fundamental unit of measurement lengthwise is meter (m). one nanometer is 10-9 meters (one billionth of a meter). as shown in Figure 1.1

One meter	= 39 inches	One inch	= 2.54 cm
	= 100 cm		= 1 hundred of a meter
	= 1000 mm		= 1 thousand of a meter
	= 1000, 000 nm		= 1 million of a meter
	= 1,000,000,000 nm		= 1 billion of a meter

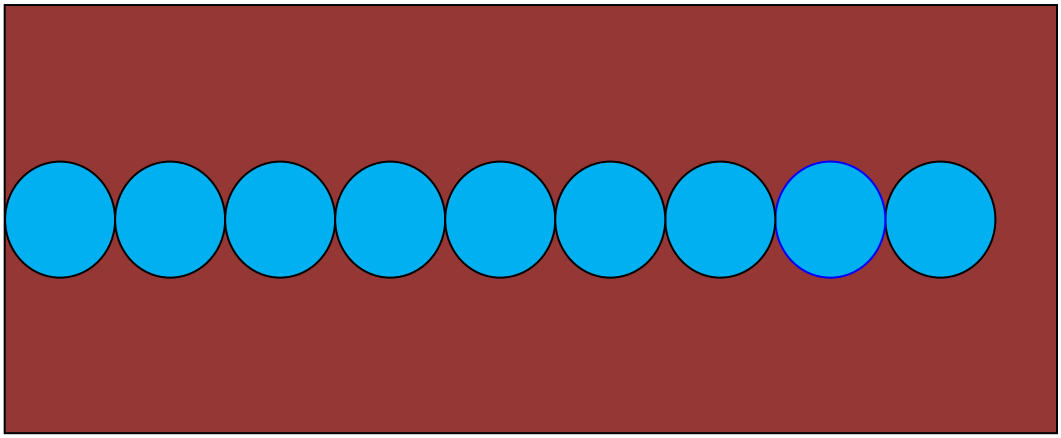

Figure 1.1. Hydrogen atoms to be found side by side to create 1 nm

Nanoscale Materials

One nanometer (nm) is one billionth of a meter and it is also equivalent to ten Angstroms. As such a nanometer is 10^{-9} m and it is 10,000 times smaller than the diameter Nanotechnology involves the manipulation of materials at millimicron sizes resulting in the fabrication of nanodevices having increased performance.of a human hair it shown in **Figure1.2**.

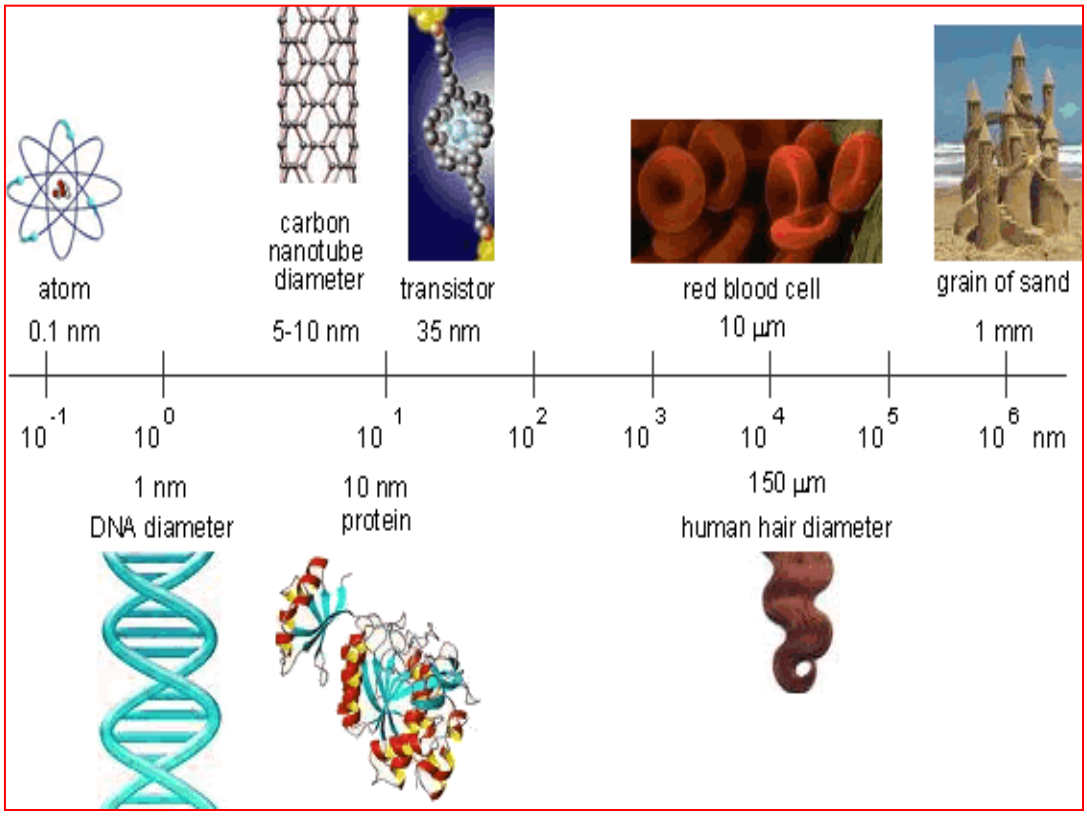

Figure1.2 Different nanoscale objects starting with atoms and molecules

MATERIALS AND METHODS

Chemicals

Tetraethoxysilane (TEOS), selenium tetrachloride, Zinc acetylcetonate, Tetraisopropyl orthotitanate, Stannous chloride pentahydrate, Indium chloride, NH_3 solution, nitric acid (HNO_3-65%), methyl green ($C_{26}H_{33}N_3Cl_2$) and ruthenium dye (535-

bisTBA, N719) were used as received. A gift sample of TiO_2–P25 (80% anatase), ethanol, t-BuOH and coumarin (1 mM of 4-hydroxycoumarin) double distilled water were the guaranteed reagents of Sigma Aldrich and used as such. The aqueous solutions were prepared by using double distilled water.

Synthesis Of Se-Doped Zno

The standard solutions Zinc and selenium precursors were made in the same way, with constant vigorous stirring. In each beaker, the precursors of ZnO were produced in Zinc acetylcetonate (0.9 M) in 75 mL of ethanol under continual stirring. Similarly, Se were produced in selenium tetrachloride (0.3 M) precursors were produced in 25 ml of ethanol in each beaker under continual stirring (solution 2 followed by 1 h of continuous stirring). Drop by drop, aqueous ammonia solution was added to it, and it was vigorously stirred for 4 hours. Finally, the gel was formed the resulting gel was prepared (Se-doped ZnO ie 1:3 ratio prepared.) were collected were calcined at 250, 500 and 600 degrees Celsius at Muffle furnace (M.F) 3h respectively. To compare the results a pure ZnO nanomaterial was created. For the sake of comparison, the study was prepared in the same via Pure (ZnO) was prepared by a similar procedure without the addition of Se.

CHARACTERIZATION METHODS

XRD Analysis

It is a non destructive technique used for the phase identification of materials. The crystal lattice is a three dimensional array of atoms in space with the lattice planes separated by a distance d. When a monochromatic X-rays fall on the crystalline surface they are scattered and gives rise to interference phenomenon. The diffracted X-rays from various planes with integral multiple (n) of wavelength (λ) will interfere constructively and results in a large output signal at the corresponding angles in the spectrum. The diffraction with half integral multiple of wavelength will interfere destructively and will cancel each other's effect. By changing the angle (θ) the lattice spacing (d) varies to satisfy the Bragg's law XRD pattern plays an important role in determining the lattice parameter and the number of planes with various orientations for powder samples. The grains in the powder samples are randomly oriented and the peak positions are used to identify the planes. The wave length of an x-ray source is known and the angle (θ) can be estimated from the XRD spectra and hence the lattice spacing (d) can be calculated using Bragg's law

$$n\lambda = 2d \sin\theta \text{ ---------- (2.1)}$$

HR-TEM

High-resolution transmission electron microscopy image was examined using a JEOL 3010 high resolution transmission electron microscope with a UHR pole piece operates at an accelerating voltage of 300 kV. The samples for TEM analysis were prepared by dispersion in ethanol under sonication and deposited on a carbon film supported on a copper grid

UV-VIS-DRS ANALYSIS

Ultra violet-visible (UV-Vis) spectroscopy offers a relatively straight forward and effective way for quantitatively characterizing both organic and inorganic compounds. Furthermore as it operates on the principle of absorption of photons that promotes the mole cute to an excited state it is an ideal technique for determining the electronic properties such as the band gap of a material. UV-vis analysis can be performed on MNPs dispersed in a solver or embedded in the insulator matrix. In such cases, absorption of incident radiations takes place due to surface Plasmon resonance (SPR) of the MNPs surface Plasmon's are essentially the wakes that are trapped on the surface because of their interaction with the free electrons of the metal. Ultraviolet and visible light absorbance spectra were measured over a range of 800-200 nm with a Shimadzu UV-1650PC recording spectrometer using a quartz cell with 10 mm optical path length.

PL Analysis

Photoluminescence spectra at room temperature were recorded using a Perkin-Elmer LS 55 fluorescence spectrometer. Nanoparticles were dispersed in chloroform and excited using light of wavelength 300 nm

Photovoltaic Measurements

The photovoltaic properties of the Dye Sensitized Solar cells (DSSC's) were characterized by recording the photocurrent voltage (I–V) curves under illumination of Xenon (Xe) light of 100W was selected to stimulate sunlight (A.M 1.5), and an I–V analyzer (Keithely 2450) was employed to measure the current against voltage.

Synthesis And Characterization Of Se-DOPED ZnO Nanocomposite Material And Its Multi Applications

Increasing concerns about the energy crisis, climate change, decreasing availability of fossil fuels and environmental issues are motivating research of sustainable and renewable energy resources [**Jacobson et al., 2009: Armarolie et al., 2004: Kalyanasundaram et al., 2010]** The key for the success of this goal lies in the development of efficient energy conversion and storage devices. Energy management, used to decouple the timing of generation and consumption of electric energy, is also fundamental for cost reduction and/or increasing income from electricity and heat generation. Thus, the possibility to achieve solar energy conversion exploiting natural pigments have been largely investigated, suggesting a cheap and simple approach based on the chemical and physical processing of these pigments, avoiding any hazardous waste by-products. In particular, vegetable pigments can be easily extracted from fruit, leaves, flowers and algae used in Dye senziteser Solar Cells (DDSSCs) [**Calogero G et al., 2010: Calogero G et al., 2008: Calogero G et al., 2010: Calogero G et al., 2014]**. All though, many other Transparent conducting films (TC) materials have also been proposed as window electrode for Dye senziteser Solar Cells (DSSCs) such as doped oxide-based thin films ZnO/Ag/ZnO, and ZnO/Cu/ZnO, etc. Fluorine Tin Oxide (FTO) is the reference transparent conductive oxides (TCO) in DSSCs because it has the highest work function (4.9eV vs 4.8eV of Indium Tin Oxide (ITO), best thermal stability, mechanical and chemical durability associated with the least toxicity and most of all the lowest cost with respect to all for mentioned materials [**Huang et al., 2006: Huang et al., 2007: Gordon et al., 2000**]. Dye from industrial effluents is frequently a significant environmental issue. Different dyes have been employed in the textile, dyeing, paper, pulp, plastic, leather, cosmetics, and food industries, and the coloured dyestuff released by these industries poses significant health and environmental risks [**Arikan et al., 2004: Liquiang et al., 2003**]. Metal oxide NPs such as ZnO, TiO_2, SnO_2 were widely studied for their potential application in the field of electronics, sensors, optoelectronic, photocatalysis etc [**Bargougui et al., 2014: Banyamin et al., 2014: Talari et al., 2012**] Selenium is found in nature in small quantities, what results in its high price. In large industrial furnaces, from the selenium added to the initial composition of the batch, almost 80% volatilize, and the remaining may form colorless selenium. The Se-doped ZnO can play an important role in various applications because of remarkable health and biological, photodegradation, photo-conductive application [**Samuel Marcio et al., 2015: Sowbhagya et al., 2014**]. In this paper Se-doped ZnO nancomposite material have been synthesized via sol–gel method and their structural, morphological, Photocatalytic and electrochemical application are reported

Evaluation Of The Observations

XRD Analysis

Figure 3.1 XRD analysis of ZnO and Se/ZnO nancomposite material displayed in exhibit different peaks at angles 2Θ of ≈ 31.9°,34.6°, 36.4°, 47.8°, 56.8°, 64.1°, 66.7°, 68.1°, and 69.2° corresponding to the respective reflections from the (100),(002), (101), (102), (110), (103), (200), (112), and (201) crystal planes of the hexagonal wurtzite ZnO structure (JCPDS 36-1451) but no of peaks corresponding to the JCPDS 06-0362 of the Se. The concordant

XRD peaks broadening with less intensity for the Se-doped nancomposite material pattern relative to those of pristine ZnO nancomposite material is perceived.

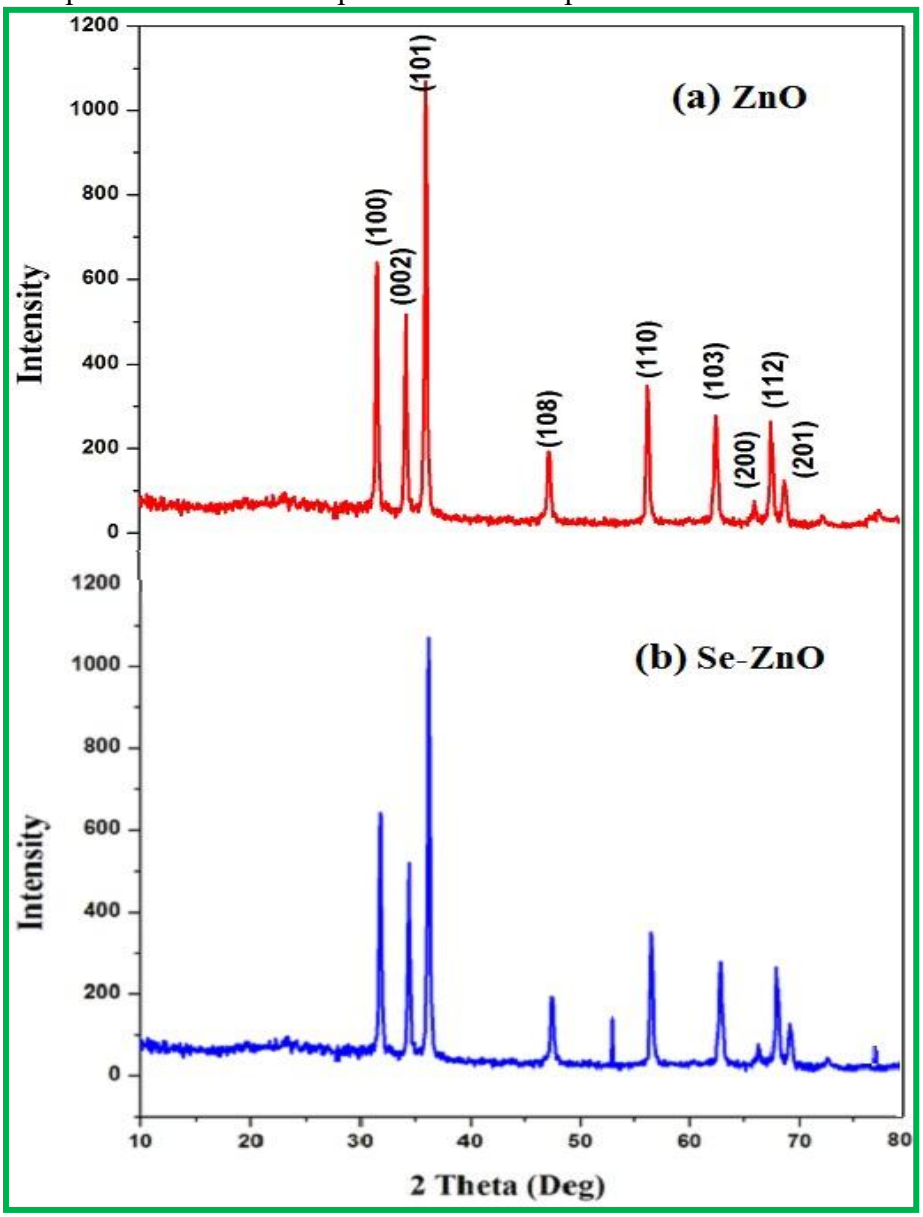

Figure. 3.1. XRD analysis of: Prepared (a) ZnO and (b) Se-doped ZnO nancomposite materials

HR-SEM

High-resolution Scanning electron microscopy (HR-SEM) is a method for high resolution imaging of surfaces. The texture and morphology of the nanocomposite are very important parameters as they influence the photocatalytic activity. **Figure 3.2 a and b** show the HR-SEM images of bare ZnO (**Figure 3.2a**) and Se-ZnO (**Figure 3.2b**) at different magnifications. The HR-SEM images of ZnO and Se- ZnO at a magnification of 10 µm are shown in **Figure 3.3 a and b**. In the HR-SEM the shape of the produced ZnO and Se-ZnO appears to be nano hexagonal flakes and wurtxite Crystal like structures was obtained. Se dispersed on the surface of ZnO and thus increasing the light utilization rate and photocatalytic activity

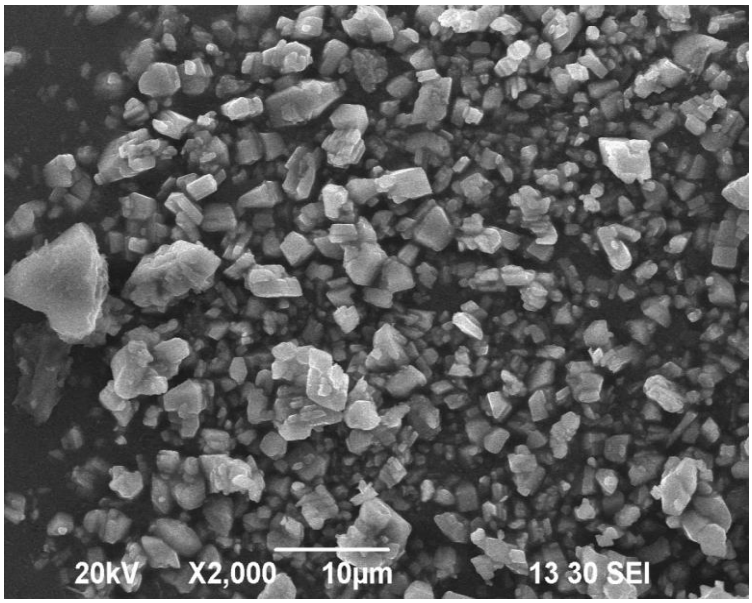

Figure. 3.2a. HR-SEM images of: Prepared ZnO nancomposite material (10 µm)

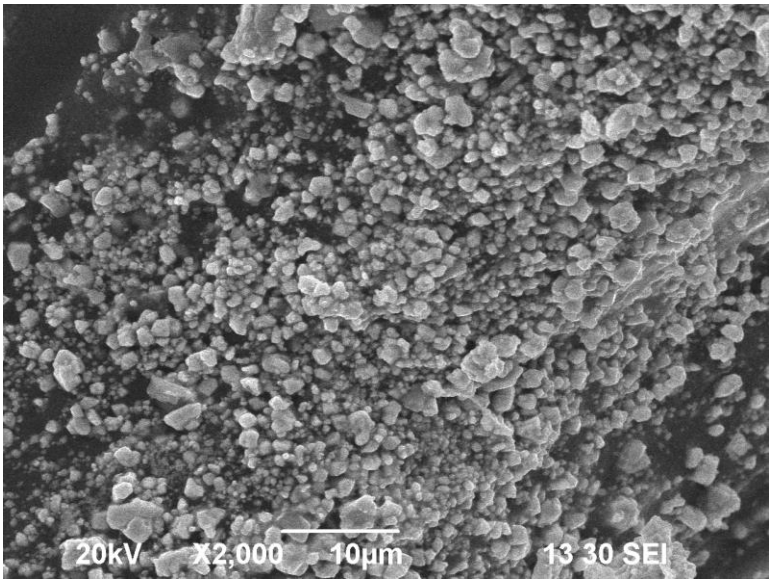

Figure. 3.2b. HR-SEM images of: Prepared Se-doped ZnO nancomposite materials (10 µm)

UV-VIS DRS SPECTRUM

UV-Vis-DRS analysis diffuse reflectance spectra analysis of ZnO and Se-ZnO nanocomposite material in are displayed (a & a1-250ºC, b & b1-500ºC and c & c1-600ºC) present showed in **Figure. 3.3**. UV–Vis spectra are transformed to the Kubelka–Munk function F(R) to separate the extent of light absorption from scattering. The band gap energy is obtained from the plot of the modified Kubelka–Munk function (F(R) E)1/2 versus the energy of the absorbed light E by the Eq. (4.1)

$$(F(R)\,E)^{1/2} = \frac{(1-R)^{1/2}}{2R} \times h\nu \quad \text{.....(4.1)}$$

The final result indicates was band gab energy of the chemical synthesis ZnO (a, b & c) and Se-ZnO (a1, b1 & c1) nanocomposite material are variation of calcination by (a & a1-250ºC [3.3 & 3.15 eV], b & b1-500ºC [3.2 & 3 eV] and c & c1-600ºC) [3.0 & 2.8 eV

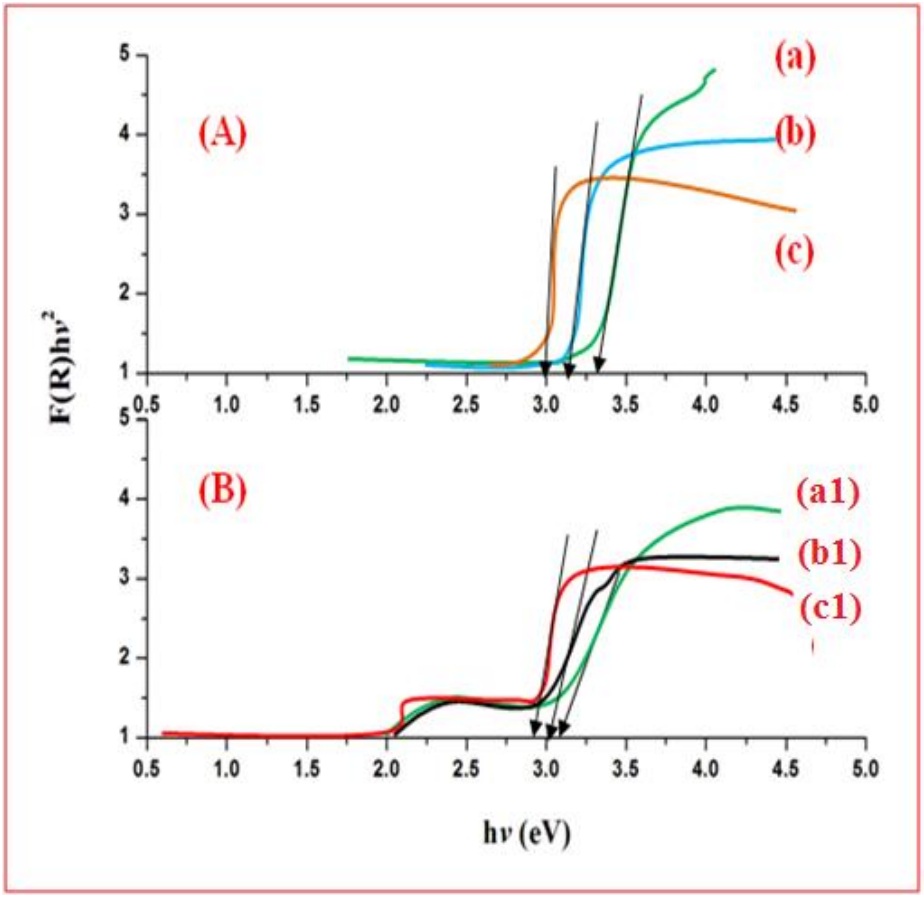

Figure. 3.3. UV-Vis DRS Band gap energy: (A) [(a) ZnO-250^{0}C, (b) ZnO-500^{0}C, (c) ZnO-600^{0}C] and (B) [(a1) Se-ZnO-250^{0}C, (b1) Se-ZnO-500^{0}C, (c1) Se-ZnO-600^{0}C] nancomposite material

PL Spectral Analysis

A **Figure. 3.4** shows are (a& a1-250ºC, b & b1-500ºC and c & c1-600ºC) present The PL spectrum of the prepared ZnO and Se-ZnO Photoluminescence occurs due to the recombination of electron-hole pair in the semiconductor. The PL spectra of nanocomposite material show that the positions of peaks are similar, but the PL intensity of Se-ZnO (Fig. (a1-250º C, b1-500ºC and c1-600ºC)) is the lower than the PL intensity of prepared ZnO. This is because of suppression of recombination of the photogenerated electron-hole pairs by the Se doped ZnO. Inhibition of electron-hole recombination makes this nanocomposite material more photocatalytic activity

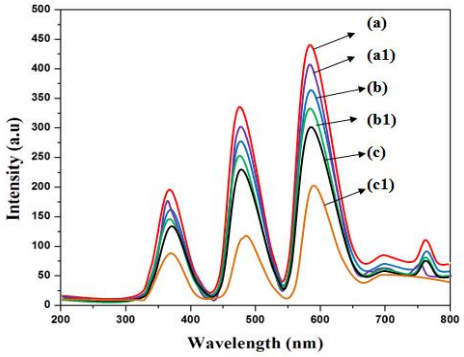

Figure .3.4. PL : (a) ZnO-250^{0}C, (b) ZnO-500^{0}C, (c) ZnO-600^{0}C and (a1) Se-ZnO-250^{0}C, (b1) Se-ZnO-500^{0}C, (c1) Se-ZnO-600^{0}C nancomposite material

Catalytic Application

Effect Of PH

Figure.3.5 shows effect of pH on the efficiency of methyl green dye degradation with repeated catalys, the photocatalytic degradation of pesticides was examined over the pH range of 3–12. The effect of pH analysis on photodegradation of MG dye compared to dye was investigated in the pH ranges of 3, 5, 7, 9, 11, and 12, with the results revealing that degradation increases with rising pH up to 7 then decreases. The percentages of MG dyedegradation after 40 minutes of UV and Solar irradiation are Se-SiO_2 active temperature 600^{o}C by [pH = 7 (95.5 percent)] and [pH = 7 (99 percent)] at respectively. For MG dye degradation, a pH of 7 is determined to be optimal. This figure demonstrates that low removal effectiveness at acidic pH ranges could be attributed to the dissolving of Se-SiO_2 nanocomposite material. The final result shows that natural solar light irradiation has a very strong photocatalytic activity that of UV-Light irradiation.

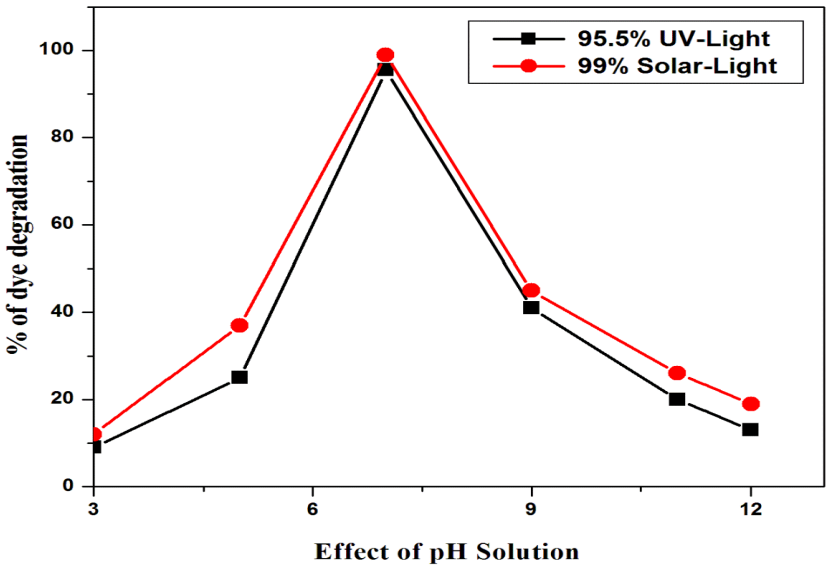

Figure .3.5. The effects of pH; Se-doped ZnO nancomposite material (a) UV and (b) Solar irradiation

Mechanism Effect

This mechanism of photocatalytic efficiency as follows

^{1} MG dye $_0$ + hν → MG dye $_1$ …(3.2)

^{1} MG $_1$ + ISC →^{3} MG dye $_1$ … (3.3)

Se-ZnO (SC) + hν → e^-(CB) + h^+(VB) …(3.4)

$^-$ OH + h^+ → $^\bullet$OH … (3.5)

$^\bullet$OH + ^{3} MG dye $_1$ → Leuco MG dye … (3.6)

Leuco MG dye → Products … (3.7)

MG dye absorbs selected wavelength photons and generates an energetic singlet state. It also travels via ISC, or intersystem crossover to give it an extra established triplet state. This energy is also used by the Se-ZnO Semiconductor or SC to excite its electron from the valence band to the conduction band. A proton can be extracted from – OH by a hole (h+) present in the semiconductor's valence ban]d resulting in ^{o}OH. The MG dye will be oxidised to its leuco form by this hydroxyl radical, which may eventually decay to products. The presence of an ^{o}OH scavenger (2-propanol) significantly reduced the rate of degradation of

MG dye indicating that ^{o}OH is an active oxidizing [Senthilvelan et al., 2015] species in the degradation of MG dye Shown in SCHEME.3.1

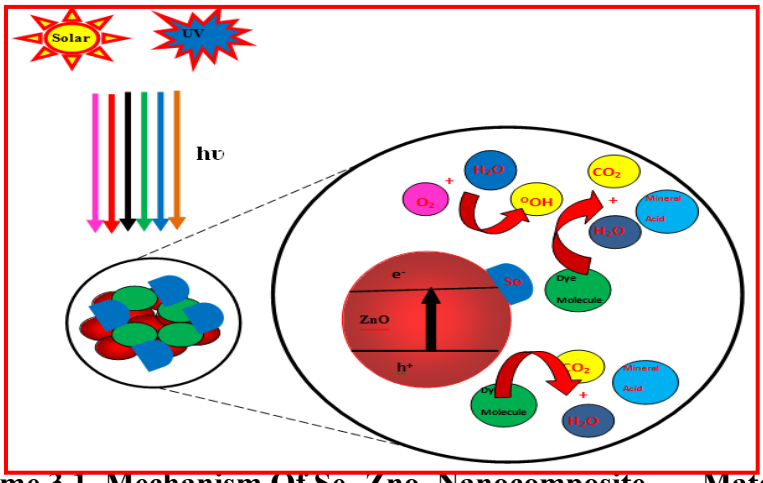

Scheme 3.1. Mechanism Of Se- Zno Nanocomposite Material.

Chemical Oxygen Demand Analysis (Cod)

The COD analysis of MG dye on mineralization of ZnO and Se-doped ZnO nanocomposite material loading amount of 0.06 g on dye initial concentration ($1x10^{-4}$) suspension for 40 mL pH neutral solution and air passing with UV and Solar- light irradiation. The % of Chemical oxygen demand analysis reduction of MG % of COD reduction of ZnO [0 -40 min (37 %)] and Se-doped ZnO [0-40 min (94.5 %)] and ZnO [0 -40 min (45 %)] and Se-doped ZnO [0-40 min (98 %)] of COD analysis measurements reduction is obtained. The mineralization is also specific by formation of calcium carbonate when the evolved gas (Carbandioxide) through photodegradation is accepted and calcium hydroxide is obtained. The final result indicate solar-light irradiation high efficiency of reduction that UV-Light irradiation its show in **Figure. 3.6 (a and b).**

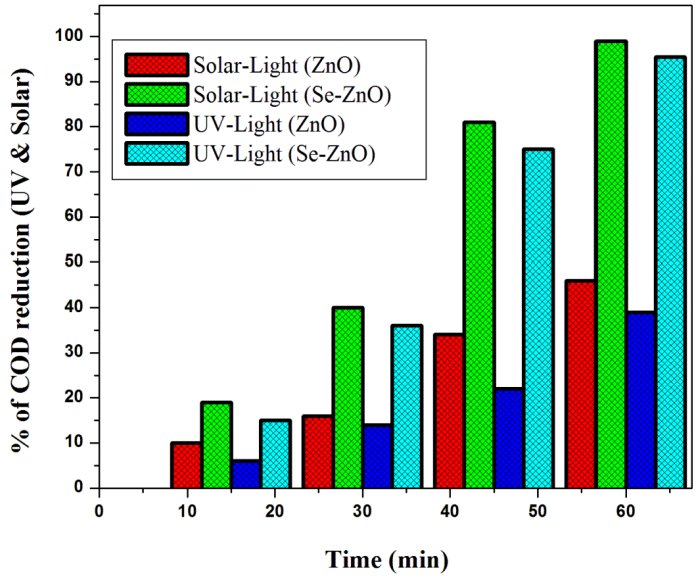

Figure. 3.6. COD analysis of (a) ZnO and (b) Se-doped ZnO nanocomposite material under UV and Solar-Light irradiation

Antibacterial Activity

Table 3.1. Antibacterial activity against Gram-positive and Gram-negative bacteria by disc diffusion method

S. No.	Bacteria	Standard antibiotic* disc	Zone of inhibition (mm)		
			1 [ZnO]	2 [Se- ZnO]	Control (DMSO)
1	*Staphylococcus aureus* (Positive)	31	17	28	19
2	*Escherichia coli* (Negative)	34	18	29	16

***Ciprofloxacin**

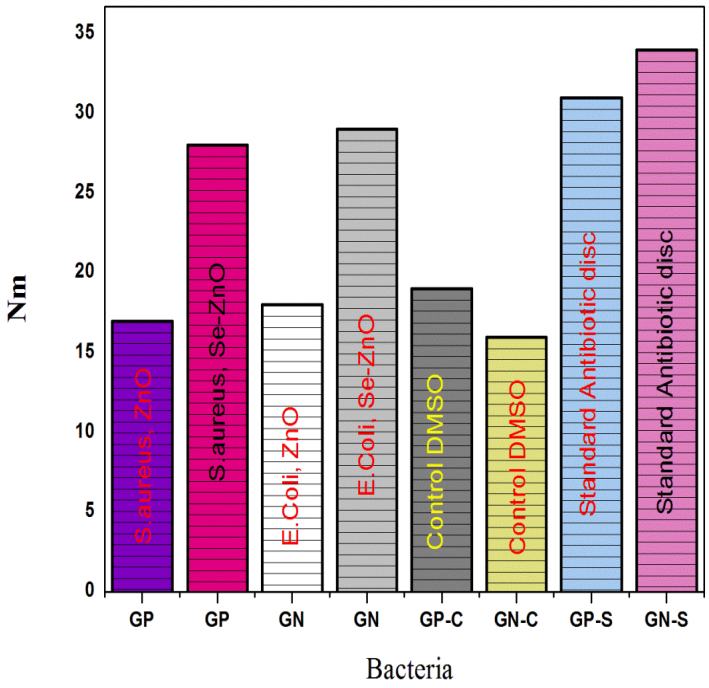

Figure.3.7. Bacterial Strains: (a) *E.coli*, (b) *S. aureus* research of ZnO nanopowder and Prepared Se doped ZnO nanomaterial

SUMMARY AND CONCLUSIONS

Five modified semiconductor photocatalysts Se-doped ZnO have been prepared and characterized by high resolution scanning electron microscope (HR-SEM), energy dispersive spectra (EDS), high resolution transmission electron microscope (HR-TEM), X-ray diffraction (XRD), diffuse reflectance spectra (DRS) and photoluminescence spectra (PL) analysis.

Photocatalytic degradation of Methyl Green dye using the catalysts Se-doped ZnO, under UV and solar irradiation have been investigated. The results are discussed in chapters 3 to 7. Based on the results the following conclusions have been drawn.

- HR-SEM images of Se-doped ZnO shows the hexagonal flakes and wurtxite Crystal like structures.
- The EDS of Se-doped ZnO shows the presence of Zn, Se and O in the catalyst.
- HR-TEM images of Se-doped ZnO shows the presence of spherical shaped structures
- UV-DRS ; Prepared Se-doped ZnO (3.6 eV) lower band gab energy enhanced photocatalytic activity that of ZnO (4.5 eV)

- Photoluminescence intensity of Se-doped ZnO is less than prepared ZnO, which indicates the inhibition of recombination of the photogenerated electron-hole pairs by the Se-doped ZnO.

REFERENCE

1. Banyamin Z.Y, Kelly P.J, West G, Boardman (2014) J, Coatings, , 4,732–746.
2. Bargougui R, (20140) J. Mater. Sci. Mater. Electron. 25, 2066–2071.
3. Calogero G and Di Marco G (2008) *Sol. Energy Mater. Sol. Cells.* 92, 1341-1346
4. Calogero G, Bartolotta A, Di Marco G, Di Carlo A and Bonaccors F (2014) RSC, 9, 1-75,
5. Calogero G, Di Marco G, Cazzanti S, Caramori S, Argazzi R, Di Carlo A, Bignozzi C. A, (2010) *Int. Jour. of Mol. Sci.* 11, 254-267.
6. Calogero G, Yum J-H, Sinopoli A, Di Marco G, Gratzel M, Nazeeruddin M. K, *So Energy* 2012, 86, 1563-1575. https://doi.org/10.1016/j.solener.2012.02.018
7. Dye Sensitized Solar Cells, edited by K. Kalyanasundaram, EPFL press, Lausanne, Switzerland, CRC Press, Hardcover. 1, 320
8. Energia oggi ieri e domain (2004) Bonomia University press - Armarolie N. Balzani V. (ISBN 88-7395-093-0)
9. Gordon R.G (2000) MRS Bulletin, 25, 52-57,
10. Gulnaz O, Kaya A, Matyar F and Arikan B, J (2004) Hazard. Mater. 108, 183–188.
11. Langner B. E, in: Ullmann's Encyclopedia of Industrial Chemistry 2000. Print ISBN: 9783527303854, Online ISBN: 9783527306732, DOI: 10.1002/14356007.
12. Liquiang J, Xiaojun S, Jing S, Weimin C. and Zili (2003) Sol. Energy Mater. Sol. Cells.70, 133–151.
13. Renata Andrade K, Samuel Marcio T (2015) Sol-Gel Method Materials Science Forum, , 805, 564-569.
14. Sabri N.S, Mohd Deni M.S, Zakaria A, Talari M.K (2012) Phys. Proc., 25, 233–239.
15. Sahu D. R and Huang J-L (2007) Thin Solid Film, 516, 208-211.
16. Sahu D. R, Lin S-Y and Huang J-L (2006) Appl. Surf. Sci. 252, 7509-7514.
17. Sowbhagya S, Ananda (2014) Am. Chem. Sci. J. 4, 616–637.